Content list available at ICONSMAT

Journal of Construction Materials

Journal homepage: www.iconsmat.com.au/publication

Article history:
Received 22 October 2021
Received in revised form
6 November 2021
Accepted 6 November 2021
Available online 6 November 2021

Evaluation of corrosion in steel reinforced concrete with brick waste

Julieta D. Chelaru*[1], Maria Gorea[1]

[1] Chemical Engineering Department, Faculty of Chemistry and Chemical Engineering, Babes-Bolyai University, Cluj-Napoca, RO 400028, Romania.

*Corresponding author: phone: 40-264-593833; fax: 40-264-590818; e-mail: julieta.chelaru@ubbcluj.ro

Abstract

The massive demolition of old buildings in recent years has generated tons of waste, especially brick waste. Thus, a concern of recent research is the use of this waste for the production of environmentally friendly concrete. At the same time, corrosion of the reinforcement steel rebar in classical concrete is a current problem. In this context, in the present paper a study was carried out on the corrosion of metal reinforcement in cement mortars with added brick waste. The corrosion process was analyzed on four compositions of mortars without and with 15%, 25% and 35% brick waste replacing the sand. The brick waste has majority content in SiO2, Al2O3, FeO3 and CaO. The grain size distribution of brick waste was close to that of the sand (d_{max} = 2 mm). The preparation method of the samples was similar to ordinary mortars. The corrosion action on the rebar in concrete, at different brick waste concentrations, was investigated by electrochemical measurements (polarization curves and electrochemical impedance spectroscopy (EIS)) at 1 month and 26 months. The results obtained at 26 months revealed that the addition of the brick waste in mortar improved the anticorrosion properties in the case of all samples compared with the etalon mortar. The best results were obtained in the case of the sample with 15% brick waste (the efficiency was ≈ 90%). The corrosion intermediary layer formed on the rebar surface was evidenced by SEM-EDX.

DOI: 10.36756/JCM.v3.1.3

Keywords

EIS, steel corrosion, steel reinforced concrete, waste materials.

Introduction

Corrosion of steel rebar is the main cause of failures of reinforced concrete [1]. Because reinforced concrete is one of the most used materials in the field of buildings, its destruction involves significant financial losses. On the other hand, the massive generation of the waste from building by demolitions is a large subject in the recent years [2], [3]. A sustainable development of modern society involves its reducing by recycling. Lately, a lot of research focused on the use of waste from civil construction to replace sand or aggregates in different proportions [2-5]. Also, a current concern of research is to find innovative solutions for protection against corrosion of reinforcements with low economic and low environmental impact [6-10]. In this context, the aim of this paper is to investigate the corrosion of steel rebar in mortar prepared with different concentrations of brick waste (0%, 15%, 25%, and 35%). The corrosion behavior of the steel rebar in these mortars at different concentrations of brick waste was investigated by electrochemical methods (polarization measurements and EIS). Other relevant areas of research that are focused on optimizing the construction and demolition waste management with the help of modern managerial approaches and robotics can also benefit from the outcomes of the current paper [11-20].

The Scanning Electron Microscopy (SEM) with Energy Dispersive X-ray Analysis (EDX) was used to illustrate the intermediary layer formed on the rebar surface.

Materials and methods

Mortar Samples' Composition

The four compositions of mortar without and with 15%, 25% and 35% brick waste (BW) were studied. The BW, having composition as shown in Table 1, was collected from an old, demolished building in Cluj-Napoca, Romania.

Table 1 - Chemical composition of BW

Oxide	SiO_2	TiO_2	Al_2O_3	Fe_2O_3	CaO	MgO	Na_2O	K_2O
%wt	64.86	0.54	18.0	5.19	4.62	1.6	0.95	2.5

Loss of ignition = 1.74%

The BW contains a high percentage of SiO_2 (64.86%) and alumina oxide (18%) along to alkaline-earth oxides (CaO, MgO) and alkaline oxides (Na_2O, K_2O). Alkaline-earth oxides and alkaline oxides can be solubilized in aqueous solutions increasing the pH of the system. Increasing the pH of the system leads to corrosion protection of the reinforcement.

The experimental mortars were prepared in a laboratory cement mixer. The composition of the mortar samples is shown in Table 2.

Table 2 - Composition of tested samples

Sample	Cement (%)	Sand (%)	BW (%)	Water (mL)
S0	25	75	-	225
S15	25	60	15	225
S25	25	45	25	225
S35	25	30	35	225

Figure 1 - The mortar samples. Left: General view, Right: Cross sectional view

The raw mortar samples were poured into metallic molds with 40 mm x 40 mm x 160 mm in size. The steel rebar with 6 mm diameter was embedded in middle of mortar samples (Figure 1). The samples molds with mortar were maintained in RH 95% during 24 hours. For the corrosion tests, the samples were removed from the mold and cured in humidity atmosphere.

Electrochemical Tests

The corrosion behavior of steel rebar was investigated at 1 month and 26 months. Before and between the electrochemical measurements, the samples were maintained in a humid atmosphere (RH 55%). In order to ensure conductivity between the electrodes, before the corrosion tests, the samples were immersed in electrolyte (NaCl 3%). The electrochemical corrosion measurements were performed on a PC-controlled electrochemical analyzer PAR 2273 (Princeton Applied Research, USA) using a three electrodes cell containing a working electrode (WE - rebar with an exposed area of 9.5 cm^2), a saturated Ag/AgCl/KCl electrode as reference electrode, and a Pt counter electrode.

The open circuit potential (OCP) for WE immersed in the corrosive solution was monitored for 1 hour. Then, EIS spectra were recorded in the frequency ranging from 10 kHz – 10 mHz with a disturbance voltage of ± 10 mV at 30 points/decade. The impedance data were fitted with R(QR) and R(CR)W equivalent electrical circuits, using the ZSimpWin V3.21 software. Immediately after the EIS measurement, the potentiodynamic polarization curves were recorded by scanning in a potential range of ± 20 mV and of ± 200 mV vs. OCP (for Tafel interpretation) with a scan rate of 0.166 mV/s. The testing temperature was 21 °C ± 2 °C.

SEM-EDX Analysis

SEM analysis was performed with a Scanning Jeol JEM5510LV (Japan) coupled with Oxford Instruments EDX Analysis System Inca 300 (UK) at 15 kV and spot size 39 µm.

Results and discussions

Corrosion test

In order to determine the corrosion behavior of steel rebar in different compositions of mortar, the experiments were started with recording the OCP of the samples in time. The OCP was measured vs. Ag/AgCl/KClsat and become relatively constant after one hour. The OCP values were situated between -425 mV and -492 mV for samples preserved in humid conditions for 1 month, respectively between -6 mV and -81 mV for samples preserved for 26 months.

Electrochemical Impedance Spectroscopy (EIS)

The EIS plots were recorded immediately after OCP in order to investigate the behavior corrosion of steel rebar in different compositions of mortar. The results are presented in Figure 2. The Nyquist plots for samples that were maintained for 1 month in humid conditions indicated that the impedance spectra exhibit one depressed capacitive loop (Figure 2 (a)). The impedance spectra were analyzed for all samples by fitting the experimental data with an equivalent electrical circuit that contain only one R-C couple (Figure 2 (a)); R_{ct} representing the charge transfer resistance and, C_{dl} the double layer capacity, at the rebar steel | electrolyte interface. The values of C_{dl} were calculated using equation (1):

$$C = (R^{1-n} \cdot Q)^{\frac{1}{n}} \qquad (1)$$

where: Q is the constant phase element that replaced the capacitive element due to the roughness and inhomogeneities of the coatings; coefficient n represents the depressed feature of the capacitive loop in Nyquist diagram ($0 < n \leq 1$).

Analyzing the Nyquist plots in the case of samples maintained for 26 months in humid conditions, it can be noticed a completely different behavior compared with samples maintained for 1 month. The impedance spectra were analyzed for all samples by fitting the experimental data with a R(CR)W equivalent electrical circuit. The presence of Warburg impedance indicates that the electrochemical reactions are controlled by diffusion phenomenon (Figure 2 (b)). The RΩ represents the electrolyte resistance between the reference electrode and the work electrodes surface, in the case of both equivalent electrical circuits used. To understand the electrochemical process occurring at the WEs surface, the parameters for all samples were obtained by using the proposed equivalent electrical circuits. The quality of fitting procedure was evaluated by the chi squared (χ2) values, which were of the order 10^{-4}. The results are shown in Table 3.

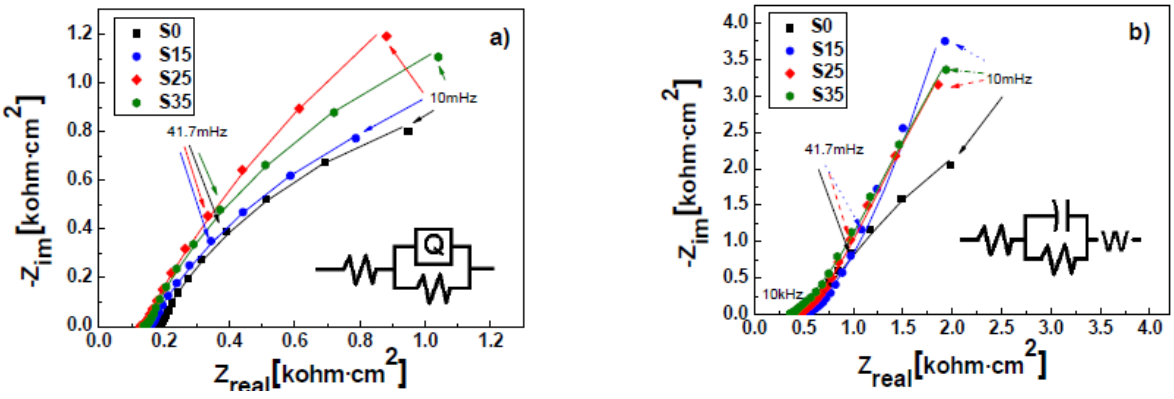

Figure 2 - Nyquist impedance diagrams for the rebar electrodes at: (a) 1 month, (b) 26 months, immersed in 3 wt.% NaCl; the lines represent fitted data

Table 3 - The electrochemical parameters

Time	S*	R_Ω(kΩ.cm^2)	Q (MF)	C (MF)	N	R(kΩ.cm^2)	W.10^4 (1/Ω.$\sqrt{Hz}$)
1 month	S0	0.179	14.21	-	0.76	2.871	-
	S15	0.154	18.95	-	0.74	3.375	-
	S25	0.132	17.20	-	0.76	7.612	-
	S35	0.142	12.13	-	0.78	4.247	-
26 months	S0	0.441	-	13.38	-	2.82	25.55
	S15	0.414	-	6.69	-	126	22.11
	S25	0.443	-	7.76	-	16.26	25.38
	S35	0.368	-	7.54	-	17.33	22.13

*Sample

Analyzing the data from Table 3 obtained after 1 month, it can be observed that the polarization resistance (R = R_p), which is an indicator of corrosion resistance, can be practically assimilated to the charge transfer resistance, and it is not influenced by the BW concentrations. In contrast, after 26 months, the R_p values are increased for all samples with BW. The highest R_p was observed for addition 15% BW (R_p = 126 [kΩ·cm^2]).

The Potentiodynamic Polarization Curves

To determine the corrosion current density (i_{corr}) and the corrosion potential (E_{corr}), the potentiodynamic polarization curves were recorded in the potential range of ± 200 mV vs. OCP (Figure 3).

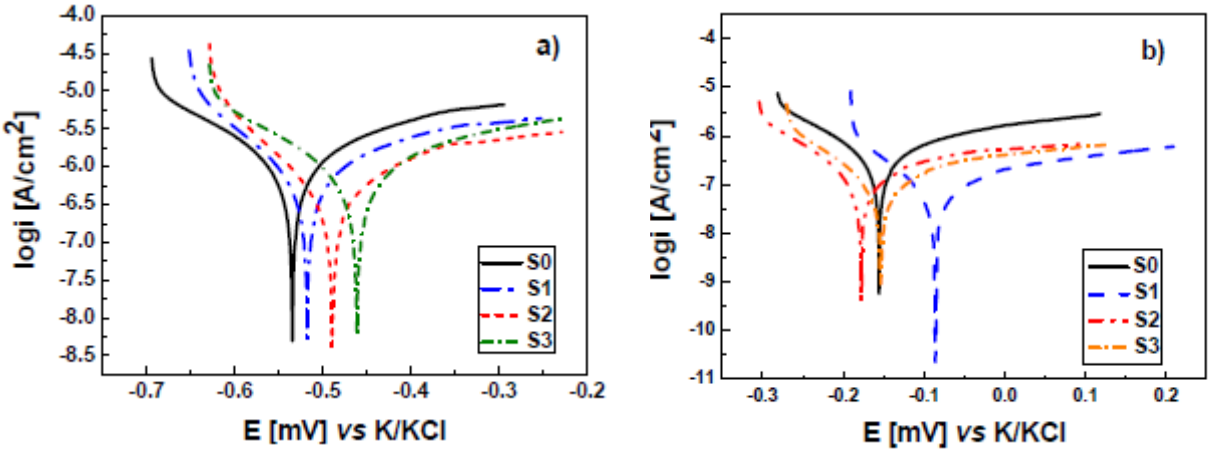

Figure 3 - Polarization curves (± 200 mV vs. OCP) recorded for rebar imbedded in mortar: (a) 1 month and (b) 26 months.

For all mortar samples, the results obtained by Tafel interpretation of the polarization curves are presented in Table 4. Based on these results, it can be observed that after maintaining the samples in

a humid atmosphere for 1 month, the values of i_{corr} are very close in all cases. This behavior assumes that the addition of BW has no influence on the corrosion properties for a short period of time. On the other hand, analyzing the results obtained after 26 months, it can be observed that the values of i_{corr} indicated a pronounced decrease for all samples that contained BW. The highest corrosion resistance (R_P = 90.47 kΩ·cm^2) and the lowest corrosion current density (i_{corr} = 0.08 μA/cm^2) were noticed at 15%. concentration of BW. This agrees with the results obtained from the EIS measurements.

Table 4 - Corrosion process parameters for studied samples

Time	S*	E_{CORR}(mV)	i_{CORR} (μA/cm^2)	RP (kΩ.cm^2)	η
1 month	S0	0.179	14.21	-	0.76
	S15	0.154	18.95	-	0.74
	S25	0.132	17.20	-	0.76
	S35	0.142	12.13	-	0.78
26 months	S0	0.441	-	13.38	-
	S15	0.414	-	6.69	-
	S25	0.443	-	7.76	-
	S35	0.368	-	7.54	-

In Table 3 are presented also the values of the anticorrosion efficiency obtained by addition the BW in mortar. The efficiency in case of all concentration of BW was determined with (2):

$$\eta = \frac{i_{corr}^0 - i_{corr}}{i_{corr}^0} [\%] \qquad (2)$$

where i_{corr}^0 and i_{corr} are current density for the sample without and with BW, respectively. As it can be observed, the inhibition is pronounced for all samples with BW after 26 months maintained in humid conditions. The highest efficiency was obtained in case of 15% BW (η = 89%).

SEM-EDX Analysis

SEM-EDX analysis was used for illustrating the intermediary layer between steel rebar and mortar matrix (S0 and S15). The steel rebar samples are presented in Figure 4. Visual examination on the surface of the rebar embedded in mortar does not show corroded areas. However, the area directly exposed to the external conditions presents a severe corrosion. The results of the SEM-EDX analysis are presented in Figures 5 and 6.

Figure 4 - Rebar samples for SEM-EDX analysis

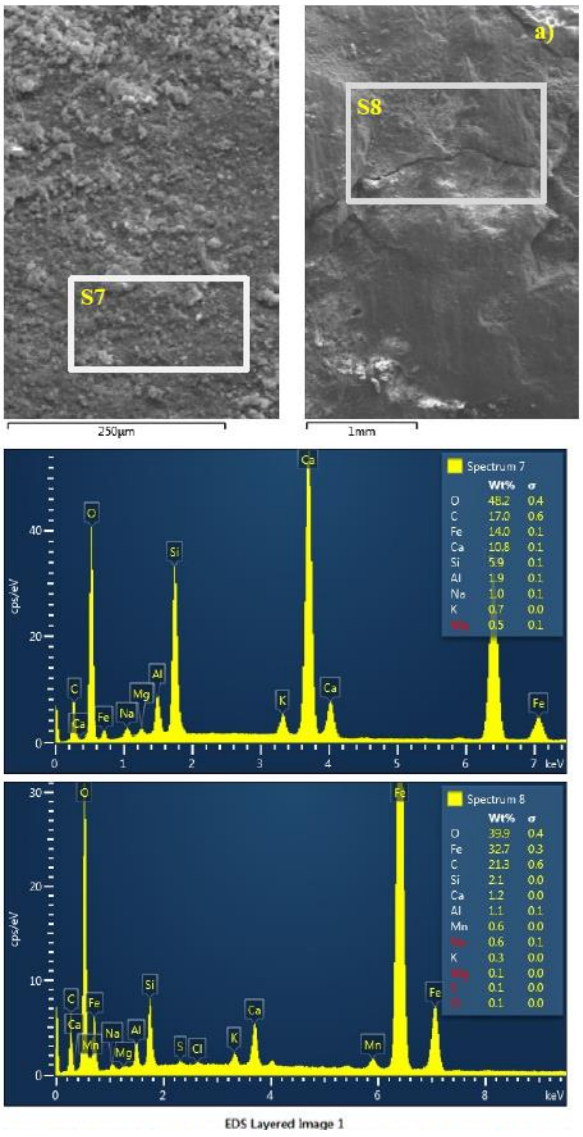

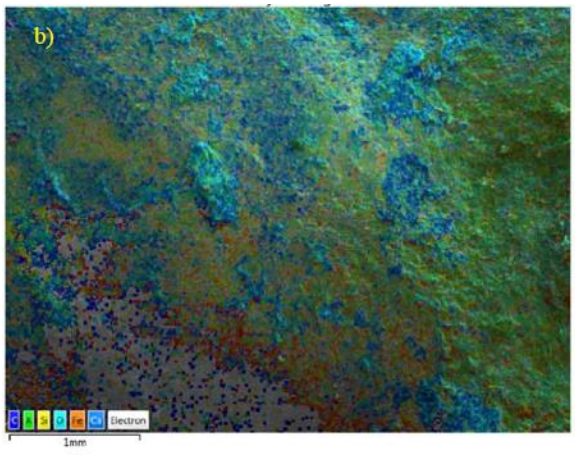

Figure 5 - SEM-EDX analysis for the S0 sample

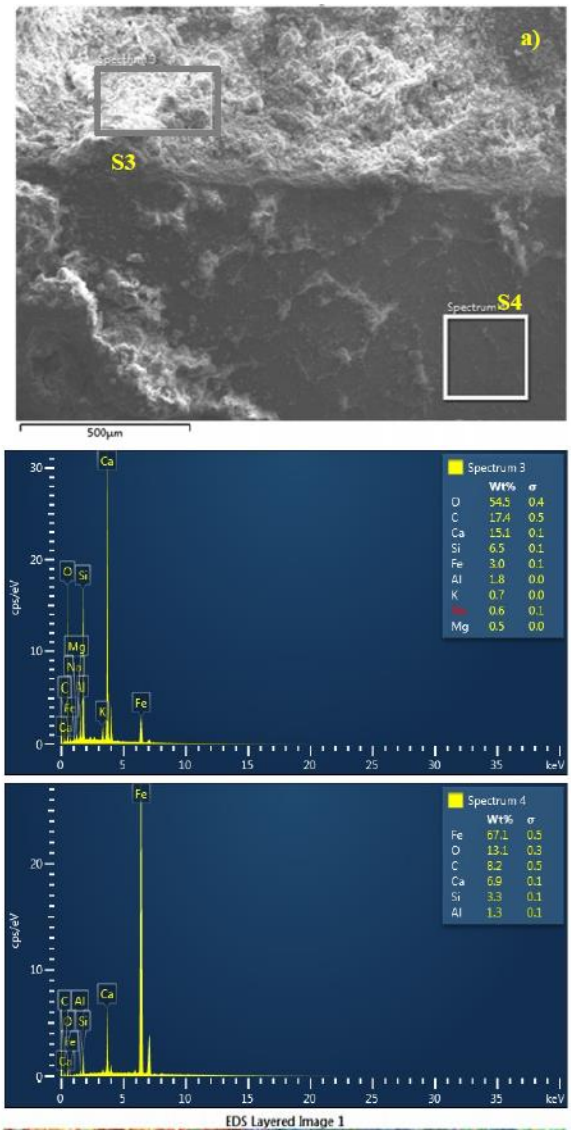

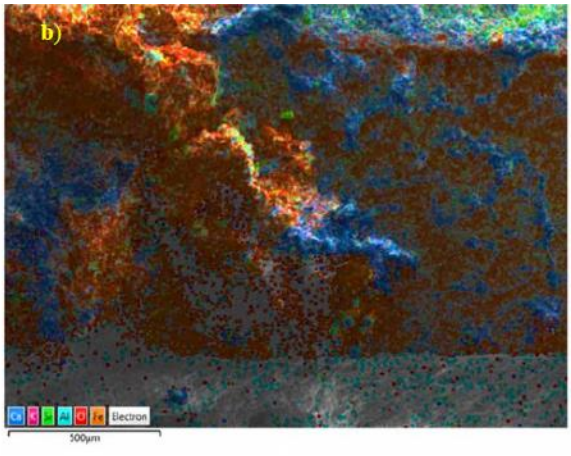

Figure 6 - SEM-EDX analysis of the S15 sample

By analyzing the distribution of elements (Figure 5 (b)) the intermediate layer between steel and concrete can be observed. Also, on the steel surface, predominate Fe and C with small amounts of Ca are observed. The presence of the Ca, in the form of hydroxide, increases the pH of the system and provides protection against corrosion to the reinforcement.

In case of the rebar embedded in concrete with 15% WB, based on the SEM-EDX the presence of a high quantity of Ca compared with the etalon concrete can be observed (0% WB). Also, the presence of alkalis which dissolve easily, maintained the pH at high values, which gives the system a good anticorrosive property. The results obtained by SEM-EDX analysis are consistent with the corrosion tests.

Conclusion and future work

Based on the electrochemical investigations (EIS and potentiodynamic polarization curves measurements), it can be concluded that in the case of the addition of the BW in the mortar composition, the anticorrosion properties of the rebar are improved. The best efficiency was noticed in case of addition 15% of BW ($\eta \approx 90\%$).

SEM-EDX analysis for rebar embedded in etalon concrete showed that the intermediary layer formed around on the rebar contains calcium hydroxide, which increases the pH of the system ensuring protection against corrosion of the reinforcement. In the case of concrete with BW, the presence of alkaline hydroxides, maintaining the pH at a high value, provides a high anti corrosion protection of the reinforcement.

The results are promising, so research will continue in the near future. Also, the corrosion behavior of the reinforced concrete with BW will be tested in petrochemical industry conditions. The corrosion test will be conducted in real residual water from the exploitation of crude oil from Transylvania, Romania.

Acknowledgement

This work was supported by a grant of the Ministry of Research, Innovation and Digitization, CNCS/CCCDI- UEFISCDI, project number PN-III-P3-3_6-H2020-2020-0058, within PNCDIIII.

References

[1] R. Rodrigues, S. Gaboreau, J. Gance, I. Ignatiadis and S. Betelu, “Reinforced concrete structures: A review of corrosion mechanisms and advances in electrical methods for corrosion monitoring”, Construction and Building Materials, Vol. 269, pp. 121240, 2021.

[2] M. Batayneh, I. Marie, I. Asi, “Use of selected waste materials in concrete mixes”, Waste Management Vol. 27, pp. 1870–1876, 2007.

[3] T. S. Serniabat, M. N. N. Khan, M. F. M. Zain, “Use of Waste Glass as Coarse Aggregate in Concrete: A Possibility towards Sustainable Building Construction”, World Academy of Science, Engineering and Technology International Journal of Civil, Environmental, Structural, Construction and Architectural Engineering vol. 8, No:10, pp.1075 – 1078, October 2014.

[4] C. Zhou and Z. Chen, “Mechanical properties of recycled concrete made with different types of coarse aggregate”, Construction and Building Materials, 134, pp. 497–506, 2017.

[5] J. D. Chelaru, F. Goga and M. Gorea, “Corrosion and mechanical properties and microstructure of cement mortar containing calcium sulphate waste”, Studia UBB Chemia, Vol. 2, pp. 271-285, 2017.

[6] V. Shubina, L. Gaillet, T. Chaussadent, T. Meylheuc, J. Creus, “Biomolecules as a sustainable protection against corrosion of reinforced carbon steel in concrete”, Journal of Cleaner Production Vol. 112, pp. 666-671, 2016.

[7] D. Erdenechimeg, T. Bujinlkham and N. Erdenepurev, “Corrosion Protection of Structural Steel by Surfactant Containing Reagents”, World Academy of Science, Engineering and Technology International Journal of Materials and Metallurgical Engineering Vol. 14, No. 1, pp. 16-19, 2020.

[8] E. J. Ruíz, J. R. Cortes and W. A. Aperador, “Evaluation of Corrosion by Impedance Spectroscopy of Embedded Steel in an Alternative Concrete Exposed to the Chloride Ion”, International Journal of Chemical, Molecular, Nuclear, Materials and Metallurgical Engineering Vol. 9, No. 3, pp. 509 – 512, October 2015.

[9] A.T. Horne, I.G. Richardson, R.M.D. Brydson, “Quantitative analysis of the microstructure of interfaces in steel reinforced concrete” Cement and Concrete Research Vol. 37, pp. 1613–1623, 2007.

[10] Y. Zhao, X. Zhang, W. Jin, “Influence of environment on the development of corrosion product-filled paste and a corrosion layer at the steel/concrete interface”, Corrosion Science Vol. 124, pp. 1–9, 2017.

[11] F. Sartipi, "Automatic sorting of recycled aggregate using image processing and object detection," Journal of Construction Materials, vol. 1, pp. 3-3, 2020, doi: https://doi.org/10.36756/JCM.v1.2.1.

[12] T. Boulos, F. Sartipi, and K. Khoshaba, "Bibliometric analysis on the status quo of robotics in construction," Journal of Construction Materials, vol. 1, pp. 2-3, 2020.

[13] F. Sartipi, "A brief critical view on the carbon-conditioning of recycled aggregate using pressure chamber," Journal of Construction Materials, vol. 2, pp. 1-4, 2020, doi: https://doi.org/10.36756/JCM.v2.1.4.

[14] A. Gharizadeh, F. Sartipi, E. Ayoubi, and A. Severino, "The chemical reactor design configuration of CO2 concrete green solution," Journal of Construction Materials, vol. 1, pp. 2-5, 2020, doi: https://doi.org/10.36756/JCM.v1.2.5.

[15] F. Sartipi, "Diffusion of Innovation Theory in the Realm of Environmental Construction," Journal of Construction Materials, vol. 1, pp. 4-2, 2020, doi: https://doi.org/10.36756/JCM.v1.3.2.

[16] F. Sartipi, A. Ghari Zadeh, and M. Gamil, "Electrical resistance of graphene reinforced cement paste," Journal of Construction Materials, 2019.

[17] F. Sartipi, "Negative interest rate: Way to tackle inflationary housing prices," Journal of Construction Materials, vol. 2, pp. 4-1, 2021, doi: https://doi.org/10.36756/JCM.v2.4.1.

[18] A. Kandiri, F. Sartipi, and M. Kioumarsi, "Predicting Compressive Strength of Concrete Containing Recycled Aggregate Using Modified ANN with Different Optimization Algorithms," Applied Sciences, vol. 11, no. 2, p. 485, 2021, doi: https://doi.org/10.3390/app11020485.

[19] F. Sartipi, "Publicizing construction firms by cryptocurrency," Journal of Construction Materials, vol. 2, pp. 3-1, 2021, doi: https://doi.org/10.36756/JCM.v2.3.1.

[20] A. Todhunter, M. Crowley, F. Sartipi, and K. Jegendran, "Use of the by-products of post-combustion carbon capture in concrete production: Australian case study," Journal of Construction Materials, 2019.